Aalto University

Aaltodoc

OPEN ACCESS

Author(s): Kalmari, Jouko & Hyyti, Heikki & Visala, Arto

Title: Sway Estimation Using Inertial Measurement Units for Cranes with a Rotating Tool

Sway Estimation using Inertial Measurement Units for Cranes with a Rotating Tool

Jouko Kalmari * **Heikki Hyyti** * **Arto Visala** *

* *Department of Automation and Systems Technology,Aalto University,*
P.O. Box 15500, 00076 Aalto, Finland (e-mail:jouko.kalmari@aalto.fi,
heikki.hyyti@aalto.fi, arto.visala@aalto.fi).

Abstract: Cranes have often a freely hanging load or tool that starts easily swaying. Anti-sway control requires that the angles and angular velocities of the swinging object are measured. Some cranes can also rotate the tool with a hydraulic motor, and in many cases this rotator angle should also be known. Instrumenting all three axes, two swaying and one rotating axis, with traditional rotary encoders can be challenging. We propose an extended Kalman filter based system using two inertial measurement units. This system can measure the swaying in both directions and estimate the rotator angle. Computer vision system is used as reference. The initial results show that the error is approximately 5 degrees in the rotator angle and 2 degrees in the sway angles. The observer runs at 100 Hz on an embedded microcontroller.

Keywords: Extended Kalman filters, inertial measurement units, observers, gyroscopes, accelerometers, sensor fusion

1. INTRODUCTION

Forest machines are complex and highly effective machines used to harvest and collect trees from forests. They are also used in other forestry tasks, such as planting and cleaning. These machines are nowadays manually operated and require skilled labor. In order to alleviate the workload, it is necessary to automate some of the work. Easy tasks have already been automated, but boom control in the forest machine is still in practice manually operated. There is therefore a need for an automatically controlled boom in forestry. However, the task is challenging, and for example Billingsley et al. (2008) state that forestry is a demanding area for robotics.

To automatically control a forest machine, the hydraulic boom and the tool have to be instrumented. The hydraulic boom is usually instrumented using linear position sensors or rotation encoders. The three-axis rotation of the tool relative to the boom is more complicated as the tool is freely hanging from the tip of the boom with a shackle and a rotator (see Fig. 1). It is challenging to instrument the shackle and the rotator angles because the tool is often in contact with different obstacles. All instrumentation has to be covered with a sturdy metal casing. This is impractical for the freely hanging shackle and for the hydraulically controlled rotator which can rotate multiple rounds around its axis. Installing joint sensors is challenging due to the mechanical structure of the shackle and the rotator.

In forest machines, the hydraulic rotator turns the tool attached to the boom. The value of the rotator angle is required in certain tasks. For example, we installed a video camera on the tool for observing tree seedlings from above. The exact camera pose was needed to use
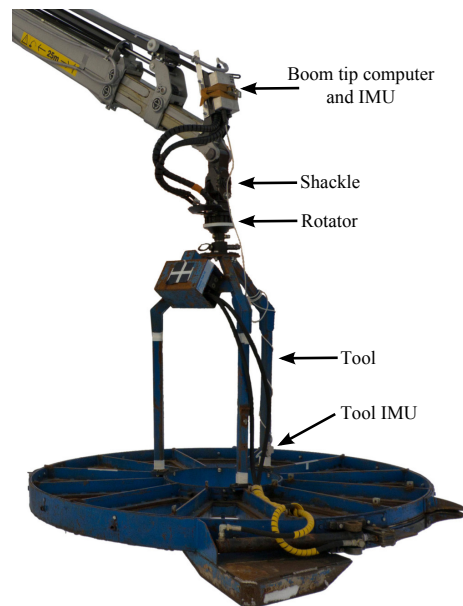

Fig. 1. The platform and instrumentation.

the extracted information. The three angles of the shackle and the rotator are required in many similar cases in which automation is introduced to machines that have a boom and a freely hanging tool attached.

In our research platform, we have a point cleaning machine attached to a hydraulic boom that we want to control automatically. The point cleaning machine is used in the weeding of young tree plants. The point cleaning machine and instrumentation are depicted in Fig. 1. The tool starts to sway when the boom is moved, but human operators are quite good at damping the swaying. To achieve good

results in automatic boom control, an anti-sway control is needed. Therefore, the swaying needs to be measured or estimated.

To ease the angle estimation and the implementation of the anti-sway control, the shackle angles are defined to be zeros when the tool is stationary. We want to measure angles in respect to the direction of gravity, not to the actual joint angles. The direction of gravity is estimated separately and the actual joint angles can be calculated from the combined results. In addition, estimates of angular velocities are required to attain a good feedback control.

There are different approaches for measuring the swaying. For example, Schaper et al. (2011) have proposed a system to measure the load position of harbor cranes using gyroscopes attached to the ropes. However, Singer et al. (1997) state that the measurement of the swaying is not required when input shaping is used. Input shaping is used as open loop control to damp the swaying for example on a gantry crane.

There are many approaches to tracking a rigid object using computer vision (Lepetit and Fua, 2005). For example, fiducial markers can be attached to the object or natural features, such as the edges or texture of the object can be used. Kawai et al. (2008) have used an image sensor to track the position of the container relative to a container crane. They use a camera pointing downwards and two landmarks attached to the spreader of the crane. The system is used only to measure only the position of the spreader.

Instead of using conventional sensors or computer vision to measure tool orientation, we use two identical inertial measurement units (IMUs). One of the units is attached to the tip of the boom and the other is attached to the tool. We use an extended Kalman filter (EKF) to estimate the angles that we are interested in.

2. METHODS

Our system (see Fig. 1) consists of a tool that is attached to a boom with a shackle and a rotator. The shackle allows the tool to sway forward and backward and left to right, and the rotator is utilized for turning the attachment.

We are using measurements from two IMUs to estimate the motion of the tool. The first IMU is installed into the tip of the boom and second on the tool itself. The second IMU needs to be installed after the rotator because we also want to measure the rotator angle. Our goal is to represent how the motion of the tip affects the motion of the tool. After we know the dynamics, we can create the Kalman filter for the estimation of the shackle and rotator angles. This observer will also estimate corresponding angular velocities.

The underlying assumption is that by comparing the accelerations and angular velocities of the tip of the boom and the angular velocities of the tool, we can estimate the pose and motion of the tool. We will also assume that the system dynamics resembles that of a pendulum with two axes and that there is some friction damping the swaying.
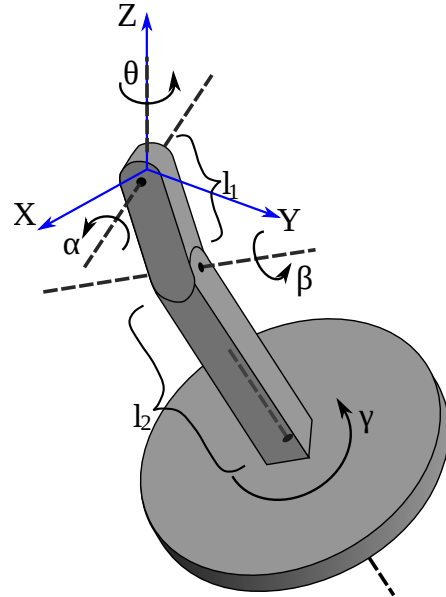

Fig. 2. Kinematic model of the system.

We are assuming that there are no external forces except gravity.

2.1 Hardware

We use two identical self-built IMUs, both of which have three-axis gyroscopes and accelerometers. Our IMUs have ADXL345 three-axis digital accelerometer and ITG-3200 three-axis digital gyroscope chips (Analog Devices (2011) and InvenSense (2010)). Both of the sensors are connected to a fast mode I2C interface, which operates at 400 kHz frequency. This sensor setup is used to calculate inertial measurements from the tool and from the boom tip. Both sensor setups are connected using separate I2C interfaces to an embedded microcontroller board (ARM Limited (2012)), where the EKF is computed at 100 Hz frequency. The estimated angles and angular velocities are finally sent to the computer controlling the boom via CAN bus.

The EKF uses angular velocities measured by the gyroscopes and accelerations measured by the accelerometers. All measurements contain gain and bias that correlates with the temperature. We performed a calibration of the gyroscope biases to remove the angular drift, which is caused by the integration of biased angular velocities. A small bias remained after the temperature compensation and calibration. The remaining small biases were removed using a bias estimator, which removed long term average from the angular velocities to minimize the drift.

IMUs were self-built because measurements from both inertial measurement units had to be combined in the EKF in real time and we need the raw angular velocity and acceleration data at high frequency. In addition, our solution is a lot more inexpensive than the solution using two commercial three-axis inertial measurement units. The downside was that the calibration was tricky and time consuming.

2.2 Kinematic description

The position and the alignment of the boom tip and the tool is presented using in total seven variables. Fig. 2 shows the basic kinematic model.

The position of the tip of the boom in respect to the world coordinate system is defined by x_b, y_b and z_b. The position of the tip of the boom is not measured directly. Instead, the accelerations of the boom tip are used. The tip is rotated by θ around the z-axis compared to the world coordinates. This new frame, called boom tip coordinate system, has z-axis pointing up, y-axis is pointing forward, and x-axis to the right.

The position of the tool relative to the boom tip is presented with three parameters α, β and γ. Rotations occur in the following order: α around x-axis, β around y-axis, and γ around z-axis (see Fig. 2). If both α and β are zero, the z-axis of tool is perpendicular to the world z-axis (i.e. the direction of gravity). Position of the mass center of the tool, or the tool position, relative to the boom tip is

$$\begin{cases} x_{tb} = -l_2 \sin(\beta) \\ y_{tb} = l_3 \sin(\alpha) \\ z_{tb} = -l_3 \cos(\alpha) \end{cases}, \tag{1}$$

where l_1 is the distance between first and second shackle axis, l_2 is the distance of the second axis and center of mass of the tool, and l_3 is:

$$l_3 = l_1 + l_2 \cos(\beta). \tag{2}$$

Position of the tool in the world coordinates can be calculated using boom tip position x_b, y_b, z_b and angle θ:

$$\begin{cases} x_t = x_b + x_{tb} \cos(\theta) - y_{tb} \sin(\theta) \\ y_t = y_b + x_{tb} \sin(\theta) + y_{tb} \cos(\theta) \\ z_t = z_b + z_{tb} \end{cases}. \tag{3}$$

The relation between the measured accelerations in boom tip coordinate system ($\ddot{x}_m$, $\ddot{y}_m$ and $\ddot{z}_m$) and the acceleration of the tip in the world coordinate is following:

$$\begin{cases} \ddot{x}_b = \ddot{x}_m \cos(\theta) - \ddot{y}_m \sin(\theta) \\ \ddot{y}_b = \ddot{x}_m \sin(\theta) + \ddot{y}_m \cos(\theta) \\ \ddot{z}_b = \ddot{z}_m \end{cases}. \tag{4}$$

The actual IMU will not always have z-axis pointing upwards. This challenge is easily corrected using a simple filter. The filter estimates the direction of the gravity using accelerometers and gyroscopes and gives the boom tip accelerations in the corrected coordinates.

2.3 Dynamics

Lagrangian dynamic formulation is utilized to solve the dynamic equations of the system. Lagrangian is the difference of kinetic and potential energy of a mechanical system:

$$L = T - V. \tag{5}$$

Any given joint torque τ_i of the system can be calculated using the Lagrangian:

$$\tau_i = \frac{d}{dt}\frac{\partial L}{\partial \dot{\theta}_i} - \frac{\partial L}{\partial \theta_i}. \tag{6}$$

The Lagrangian formulation is used for example when dynamics of a robot manipulator is constructed (e.g Craig, 2005, p. 182).

In order to use the Lagrangian formulation, the kinetic and potential energy of the system is calculated. All the mass of the system is assumed to be in one point and therefore it has no rotational inertia. If the inertial tensor of the system was taken account, the complexity of the dynamic equations would increase significantly. In our case, the angular velocities are low and we assume the rotational inertia to be insignificant.

To specify the kinetic energy of the system, the velocity of the mass in x-, y- and z-directions are calculated. The velocities are calculated by differentiating equation (3) in respect to time.

The kinetic energy of swinging mass is:

$$\begin{aligned} T &= \frac{1}{2}mv^2 = \frac{1}{2}m\left(\dot{x}_t^2 + \dot{y}_t^2 + \dot{z}_t^2\right) \\ &= 0.5m(\dot{x}_b + l_2 \sin(\beta)\sin(\theta)\dot{\theta} \\ &\quad -l_3 \cos(\alpha)\sin(\theta)\dot{\alpha} \\ &\quad -l_3 \sin(\alpha)\cos(\theta)\dot{\theta} \\ &\quad -l_2 \cos(\beta)\cos(\theta)\dot{\beta} \\ &\quad +l_2 \sin(\alpha)\sin(\beta)\sin(\theta)\dot{\beta})^2 \\ &\quad +0.5m(\dot{y}_b - l_2 \sin(\beta)\cos(\theta)\dot{\theta} \\ &\quad +l_3 \cos(\alpha)\cos(\theta)\dot{\alpha} \\ &\quad -l_3 \sin(\alpha)\sin(\theta)\dot{\theta} \\ &\quad -l_2 \cos(\beta)\sin(\theta)\dot{\beta} \\ &\quad -l_2 \sin(\alpha)\sin(\beta)\cos(\theta)\dot{\beta})^2 \\ &\quad +0.5m(\dot{z}_b + l_3 \sin(\alpha))\dot{\alpha} \\ &\quad +l_2 \cos(\alpha)\sin(\beta)\dot{\beta})^2 \end{aligned} \tag{7}$$

Potential energy of the system is dependent only of the distance of the mass in z-direction to an arbitrary reference height. From the definition of potential energy and (1) and (3) we get

$$V = mgh = mg\left(z_b - l_3 \cos(\alpha)\right). \tag{8}$$

Now the Lagrangian (6) is used to solve the torques affecting the joints. The acceleration are also substituted with (4).

$$\begin{aligned} \tau_\alpha = ml_3(\ &l_3\ddot{\alpha} \\ &+ \cos(\alpha)\ddot{y}_m + \sin(\alpha)(\ddot{z}_m + g) \\ &- 2l_2 \sin(\beta)\dot{\alpha}\dot{\beta} \\ &- l_2 \cos(\alpha)\sin(\beta)\ddot{\theta} \\ &- l_3 \sin(\alpha)\cos(\alpha)\dot{\theta}^2 \\ &- 2l_2 \cos(\alpha)\cos(\beta)\dot{\beta}\dot{\theta}) \end{aligned} \tag{9}$$

and

$$\tau_\beta = ml_2(\; l_2\ddot{\beta}$$
$$- \cos(\beta)\ddot{x}_m - \sin(\alpha)\sin(\beta)\ddot{y}_m$$
$$+ \cos(\alpha)\sin(\beta)(\ddot{z}_m + g)$$
$$+ l_3\sin(\beta)\dot{\alpha}^2$$
$$+ \sin(\alpha)(l_1\cos(\beta) + l_2)\ddot{\theta} \qquad . \qquad (10)$$
$$+ \sin(\beta)\left(l_1 - l_3\cos(\alpha)^2\right)\dot{\theta}^2$$
$$+ 2l_3\cos(\alpha)\cos(\beta)\dot{\alpha}\dot{\theta})$$

Dynamic model can be constructed by solving the angular accelerations $\ddot{\alpha}$ and $\ddot{\beta}$ from equations (9) and (10). In addition to gravitation and forces that move the tool, there are forces that damp the swaying, for example friction in the joints and drag. In fact, the second joint of the shackle assembly in our test setup is equipped with a brake preventing excess swinging. There are many models developed to describe friction (see for example Olsson et al. (1998)). We are using the viscous friction model where the force, or in our case the torque, is proportional to the angular velocity. This model does not represent accurately the real friction, but is simple to use and requires identification of only one parameter per joint. As the mass of the tool is assumed to be constant, it is separated from the friction parameters b_α and b_β. Now the torques that damp the swaying can be expressed as:

$$\begin{cases} \tau_\alpha = -b_\alpha m\dot{\alpha} \\ \tau_\beta = -b_\beta m\dot{\beta} \end{cases} \qquad . \qquad (11)$$

2.4 Extended Kalman Filter

Extended Kalman filter (EKF) is used as the actual observer. The usage of the EKF requires that inputs u, states x and measurements y are selected. The EKF is based on the dynamic model of a system presented in the following way:

$$\begin{aligned} \mathbf{x}(k+1) &= \mathbf{f}\left[\mathbf{x}(k), \mathbf{u}(k)\right] \\ \mathbf{y}(k) &= \mathbf{h}\left[\mathbf{x}(k), \mathbf{u}(k)\right] \end{aligned} \qquad (12)$$

Note the inclusion of controls in the measurement function $\mathbf{h}\left[\mathbf{x}(k), \mathbf{u}(k)\right]$.

The dynamic model constructed from equations (9), (10) and (11) is in continuous time. The discrete equivalents for these equations are determined using the Euler approximation. The discretization step is chosen to be $\Delta t = 0.01s$. As a consequence, the main loop of our filter will be running 100 Hz in the embedded controller.

As our primary goal is to measure the shackle angles α and β, and rotator angle γ, these are natural choices for states. As the dynamic equations are of second degree the angular velocities $\dot{\alpha}$ and $\dot{\beta}$ are also required in the state vector. The state vector is:

$$\mathbf{x} = \begin{bmatrix} \alpha & \beta & \gamma & \dot{\alpha} & \dot{\beta} \end{bmatrix}^T \qquad (13)$$

Some of the actual measurements of a system can be introduced as inputs or controls to the system, not used as measurements. Our goal is to keep the state vector and matrix sizes as small as possible. Thus, the measurements that are in the dynamic equations will be chosen as

inputs. These inputs are the accelerations, the angular velocity and angular acceleration of the boom tip. Also, the measured tool rotation around z-axis is chosen as an input to the system. The control vector is:

$$\mathbf{u} = \begin{bmatrix} \ddot{x}_m & \ddot{y}_m & \ddot{z}_m & \dot{\theta}_m & \ddot{\theta}_m & \dot{\gamma}_m \end{bmatrix}^T \qquad (14)$$

The angular velocities $\dot{\alpha}$ and $\dot{\beta}$ can not be measured directly as the second IMU is attached to the tool turned by the rotator. The angular velocities measured by the second IMU are called ω_x, ω_y and ω_z. These angular velocities can be presented as a function of the angles and angular velocities of the system using the following relations:

$$\begin{cases} \omega_x = & \omega_1\cos(\gamma) + \omega_2\sin(\gamma) \\ \omega_y = & -\omega_1\sin(\gamma) + \omega_2\cos(\gamma) \\ \omega_z = \dot{\gamma}_m = & \dot{\gamma} + \sin(\beta)\dot{\alpha} + \cos(\alpha)\cos(\beta)\dot{\theta} \end{cases} , \qquad (15)$$

where unrotated angular velocities of the tool, ω_1 and ω_2, are calculated using:

$$\begin{cases} \omega_1 = \cos(\beta)\dot{\alpha} - \cos(\alpha)\sin(\beta)\dot{\theta} \\ \omega_2 = \dot{\beta} + \sin(\alpha)\dot{\theta} \end{cases} . \qquad (16)$$

The first two lines in the equation (15) are used as the measurement in the extended Kalman filter. The third line is incorporated into the state model of the filter.

Now the state model, $\mathbf{f}\left[\mathbf{x}(k), \mathbf{u}(k)\right]$, used in the Kalman filter is:

$$\begin{cases} x_1^* = x_1 + \Delta t x_4 \\ x_2^* = x_2 + \Delta t x_5 \\ x_3^* = x_3 + \Delta t\left(u_6 - \sin(x_2)x_4 - \cos(x_1)\cos(x_2)u_4\right) \\ x_4^* = x_4 + \Delta t(-b_\alpha/l_3^2 x_4 + \sin(x_1)\cos(x_1)u_4^2 \\ \qquad + (-\cos(x_1)u_2 - \sin(x_1)(u_3 + g) \\ \qquad + 2l_2\sin(x_2)x_4 x_5 + l_2\cos(x_1)\sin(x_2)u_5 \\ \qquad + 2l_2\cos(x_1)\cos(x_2)x_5 u_4)/l_3) \\ x_5^* = x_5 + \Delta t(-b_\beta/l_2^2 x_5 + (\cos(x_2)u_1 \\ \qquad + \sin(x_1)\sin(x_2)u_2 - \cos(x_1)\sin(x_2)(u_3 + g) \\ \qquad - l_3\sin(x_2)x_4^2 - \sin(x_1)(l_1\cos(x_2) + l_2)u_5 \\ \qquad - \sin(x_2)(l_1 - l_3(\cos(x_1))^2)u_4^2 \\ \qquad - 2l_3\cos(x_1)\cos(x_2)x_4 u_4)/l_2) \end{cases} , \qquad (17)$$

where $l_3 = l_1 + l_2\cos(x_2)$.

The measurement model $\mathbf{h}\left[\mathbf{x}(k), \mathbf{u}(k)\right]$ is:

$$\begin{cases} y_1 = (\cos(x_2)x_4 - \cos(x_1)\sin(x_2)u_4)\cos(x_3) \\ \qquad + (x_5 + \sin(x_1)u_4)\sin(x_3) \\ y_2 = -(\cos(x_2)x_4 - \cos(x_1)\sin(x_2)u_4)\sin(x_3) \\ \qquad + (x_5 + \sin(x_1)u_4)\cos(x_3) \end{cases} . \qquad (18)$$

The time indexing of the states and measurements are left out from the (17) and (18) due to space restrictions.

Table 1. Parameters

Symbol	Name	Value
l_1	distance of 1. and 2. axle	0.22 m
l_2	distance of 2. axle and center of mass	2.09 m
b_α	1. axle friction	$0.5\frac{1}{s}$
b_β	2. axle friction	$2.0\frac{1}{s}$

Instead, a notation is used where $x_n^* = x_n(k+1)$ and $x_n = x_n(k)$.

The covariance matrices needed in the estimation process are calculated from the state and measurement functions (17) and (18) with the Jacobians :

$$
\begin{aligned}
F(k) &= \frac{\partial \mathbf{f}(k)}{\partial \mathbf{x}}|_{\mathbf{x}=\hat{\mathbf{x}}(k|k)} \\
H(k+1) &= \frac{\partial \mathbf{h}(k+1)}{\partial \mathbf{x}}|_{\mathbf{x}=\hat{\mathbf{x}}(k+1|k)}
\end{aligned}
\quad (19)
$$

The parameters of the dynamic system are presented on Table 1. Parameter l_1 is measured directly from the shackle. Rest of these parameters were estimated from the data. Kalman filter has two covariance matrices, W and V, that describe the uncertainty of the state transitions and the measurements. W and V were defined as diagonal matrices. The diagonal of the W had values: [0.000001 0.000001 0.00001 0000.1 0000.1]. The diagonal of V was: [0.01 0.01]. Greater values were given to states that were affected by the noise of the sensors.

3. RESULTS

The tests with reference measurement setup were done indoors. There were a few different tests, only one of which is presented in this chapter. The boom was moved left, right, up and down. The point cleaning machine, which was used as the swaying tool, was lowered to the ground four times.

Reference data were collected using two computer vision cameras having a frame rate of 17.4 frames per second. 297 images from one camera were selected as the basis for the reference data. In each image a certain set of clearly visible points were manually clicked and a model of the point cleaning machine was fitted to the data. A single frame of the reference image data is shown in Fig 3. We estimate that the accuracy of the reference measurement is less than 2°.

The results presented here are calculated off-line in Matlab using the IMU data collected in the tests. All the states of the estimator had initial values set to zeros. The initial state covariance matrix was a diagonal matrix with large value on the rotator angle covariance, and lower value on the other ones. This was due to the assumption that there was large uncertainty in the rotator angle.

Fig. 4 shows the estimated rotator angle and the reference. After the estimate has converged at around 70 seconds, the difference between estimate and reference is around -6° to 5°. If the transitions, where the tool rotates quickly, are not taken into account, the error is from -5° to 3° after the convergence. First two swaying happening at 21.5 - 43.6 s and 55.8 - 70.3 s are highlighted.
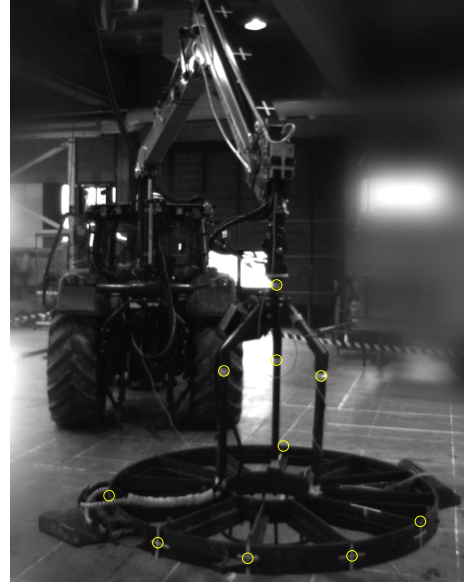

Fig. 3. A single frame used in the reference measurement. Manually selected markers are shown.
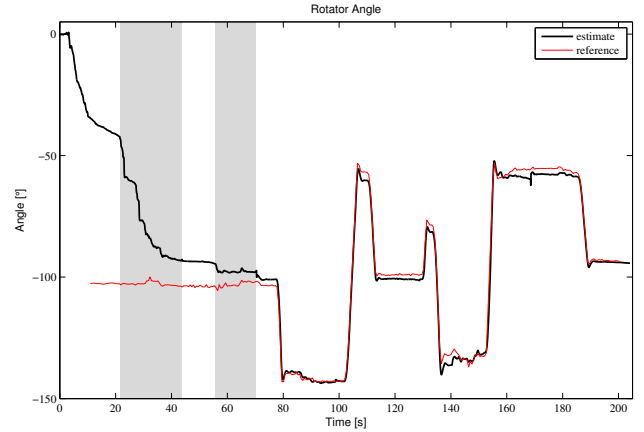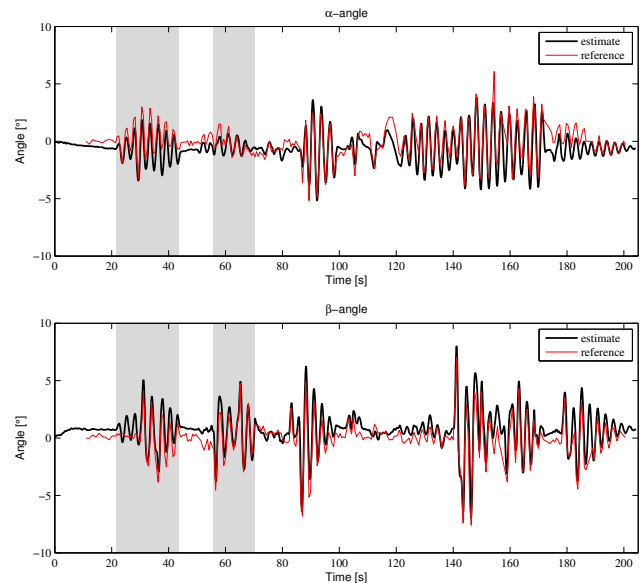

Fig. 4. Estimated rotator angle and a reference.

Fig. 5. Estimated shackle angles α and β with a reference.

Fig. 5 depicts the estimated shackle angles α and β. When the estimated angles are compared to the reference, there is often a difference of 1-2°. However, the timing and amplitude of the signals match very well. The swaying of the tool is quite modest, the maximum amplitudes of the estimated α- and β-angles are 9.0° and 14.8° respectively.

4. DISCUSSION

The estimated rotator angle in Fig. 4 shows that the results are very promising. It is important to notice that if there is no motion in the system, there is no new information for the filter, and the rotator angle estimate starts to drift. The amount of drifting depends on the quality of the gyroscopic measurements. The actual swaying starts at 21.5 seconds, but the rotator angle estimate starts to converge to the correct value almost immediately after the filtering was started. We suppose that this is due to the small vibrations caused by the engine of the tractor. As soon as the tool starts to sway, the estimate starts to converge more rapidly. In our case, the accuracy of the rotator angle estimate is more than sufficient, for example to rotate the camera image shown to the driver.

Roughly speaking, the quality of the sway angle and angular velocity estimates depends on the accuracy of the rotator angle estimate. If the shackle angles and angular velocities are used in feedback control, small errors in the measurements should not be a problem. Fig. 5 shows that the difference between the reference and the estimate is on the same magnitude as accuracy of the reference measurement.

At the end of the measurement, α and β estimates do not converge to zero even though the boom has stopped moving. When the boom is stationary, these angles should go to zero. One possible explanation for this is the bias error in the boom tip acceleration measurements.

There are some challenges in our approach. The dynamic model for example has some drawbacks. The rotational inertia is not taken into account. If the tool is rotated when it is swaying, the gyroscopic forces turn the tool in a way that our dynamic model does not capture. In the future, a more complex model should be built and the results compared. Also, the viscous friction model utilized is quite simplistic and a more realistic one might improve the results further. The basic assumption behind our equations is that there are no external forces and the tool moves like a two-dimensional pendulum. When the tool for example hits the ground or is used to grab something, these assumptions are not valid any longer. The observer uses only the gyroscope measurements from the IMU attached to the tool. One improvement would be to incorporate the measured tool accelerations. However, this would make the Kalman filter more complex and computationally expensive.

The developed extended Kalman filter is somewhat complex. There are many multiplications and additions required as the state model and the Jacobian matrices are updated at each iteration. There is also the challenge of determining good values for the filter covariance matrices. It might be possible to implement a similar filter as a nonlinear observer, for example as a sliding mode observer.

This could simplify the estimation process and reduce the possibility of programming errors while implementing the filter on embedded hardware.

By using inertial measurements to estimate all rotation angles between the tool and the boom, we can cost-effectively and robustly instrument the tool. Inertial sensors tolerate high accelerations and can be encased inside the tool to endure mechanical stress better than conventional instrumentation would. In this paper we have shown that our solution can be quite accurate, and that it can be used in real time on an embedded measurement system.

REFERENCES

Analog Devices (2011). 3-axis digital accelerometer, adxl345. URL http://www.analog.com.

ARM Limited (2012). Mbed microcontroller. URL http://mbed.org.

Billingsley, J., Visala, A., and Dunn, M. (2008). *Handbook of Robotics*, chapter Robotics in Agriculture and Forestry, 1065–1077. Springer.

Craig, J. (2005). *Introduction to robotics: mechanics and control*. Prentice Hall.

InvenSense (2010). Itg-3200evb application note. URL http://invensense.com.

Kawai, H., Choi, Y., Kim, Y., and Kubota, Y. (2008). Position measurement of container crane spreader using an image sensor system for anti-sway controllers. In *Control, Automation and Systems, 2008. ICCAS 2008. International Conference on*, 683–686. IEEE.

Lepetit, V. and Fua, P. (2005). *Monocular model-based 3D tracking of rigid objects*. Now Publishers Inc.

Olsson, H., Åström, K., Canudas de Wit, C., Gäfvert, M., and Lischinsky, P. (1998). Friction models and friction compensation. *European journal of control*, 4, 176–195.

Schaper, U., Sagert, C., Sawodny, O., and Schneider, K. (2011). A load position observer for cranes with gyroscope measurements. In *Proceedings of the 18th IFAC World Congress 2011*, 3563–3568.

Singer, N., Singhose, W., and Kriikku, E. (1997). An input shaping controller enabling cranes to move without sway. In *ANS 7th topical meeting on robotics and remote systems*, volume 1, 225–31.